Available online at www.sciencedirect.com

ScienceDirect

Procedia CIRP 33 (2015) 520 – 525

www.elsevier.com/locate/procedia

9th CIRP Conference on Intelligent Computation in Manufacturing Engineering - CIRP ICME '14

Statistical Approach to Fiber Laser Microcutting of NIMONIC® C263 Superalloy Sheet Used in Effusion Cooling System of Aero Engines

S. Genna[a], C. Leone[a-b], B. Palumbo[c], F. Tagliaferri[c]*

[a]*CIRTIBS Research Centre, University of Naples Federico II, P.le Tecchio 80, 80125 Naples, Italy*
[b]*Department of Chemical, Materials and Production Engineering, University of Naples Federico II, P.le Tecchio 80, 80125 Naples, Italy*
[c]*Department of Industrial Engineering, University of Naples Federico II, P.le Tecchio 80, 80125 Naples, Italy*

* Corresponding author. Tel.: +39 081 7682185; fax: +39 081 7682187. *E-mail address:* flaviana.tagliaferri@unina.it

Abstract

In order to reduce thermal stress and avoid premature failure of turbine blades in the hot section of aero-engines, a diffusion cooling system is often adopted. This system is a thin sheet, with a closely spaced holes array allowing a uniform cooling of the turbine blade thanks to the evenly distributing of the cooling fluid within its wall. The holes diameters vary in the range of 0.3-1.0 mm. Furthermore, tight tolerances, perpendicular surfaces, no burr, no recast layer, are required. In order to satisfy the hole requirements, typically EDM technique is adopted. However, EDM micro-drilling needs long process time (about 20 s for hole). A promising alternative is laser trepanning. In this technique, a laser beam, with a very small focused spot, is used to make a hole by circular cutting. The hole is obtained in few seconds (<3 s). In this work a preliminary study on laser microcutting of NIMONIC® C263 sheet is presented in order to verify the possibility to adopt a low-power Yb:YAG fiber laser for the microdrilling. Linear cutting tests were carried out on NIMONIC® C263 superalloy sheet, 0.38 mm thick, using a 100 W Yb:YAG fiber laser working in modulated regime. A systematic approach based on Design of Experiment (DoE) has been successfully adopted with the aim to detect which and how the process parameters affect the kerf geometry in term of kerf width, taper angle and tolerances. The examined process parameters were scan speed, on-time, pulse duration and gas pressure. A full factorial design and ANalysis Of VAriance (ANOVA) were applied. Experimental results show the possibility to obtain kerf characterized by narrow width (<100 μm), low taper angle values (<1.8°) and small tolerance (<0.22 μm). Then, the possibility to produce in-tolerance holes was proved.

© 2014 The Authors. Published by Elsevier B.V. This is an open access article under the CC BY-NC-ND license (http://creativecommons.org/licenses/by-nc-nd/4.0/).
Selection and peer-review under responsibility of the International Scientific Committee of "9th CIRP ICME Conference"

Keywords: Laser micro machining; NIMONIC® C263 superalloy; Design of Experiment.

1. Introduction

Nowadays the development of higher-efficiency low-emission aero-engines is a difficult and multi-disciplinary task. Indeed many of the recent Gas Turbine combustor supplier efforts are devoted at increasing the flame temperature while reducing the emission levels and the pressure losses. The need to increase jet engines efficiency and power has entailed improvements in the combustion process and mainly a firing temperature raise which should, however, be limited not to expose the combustor components to temperatures higher than those allowed by the available alloys [1]. One way to protect the combustor components against extreme temperatures is to use a large number of small diameter holes (typically with a diameter D < 1.0 mm) on its surface to allow air to flow over the component and to form a cooling film. This technique is widely used for different components [2-3]. In particular, to reduce thermal stress and avoid premature failure of the turbine blades in the hot section of aero-engines, a diffusion cooling system is often placed inside the turbine blade [3]. This system is a thin sheet, with a closely spaced holes array, that allows a uniform cooling of the turbine blade thanks to the evenly distributing of the cooling fluid within its wall. The holes diameters vary in the range of 0.3-1.0 mm. Furthermore, perpendicular surfaces, tight tolerances, no burr, no recast layer, are required.

In order to satisfy the hole requirements, typically EDM technique is adopted. However, EDM micro-drilling needs

2212-8271 © 2014 The Authors. Published by Elsevier B.V. This is an open access article under the CC BY-NC-ND license (http://creativecommons.org/licenses/by-nc-nd/4.0/).
Selection and peer-review under responsibility of the International Scientific Committee of "9th CIRP ICME Conference"
doi:10.1016/j.procir.2015.06.067

long process time (it was estimated about 120 minutes for a single component, 424 holes). A promising alternative is laser drilling. Two type of laser drilling exist: percussion and trepanning laser drilling. Percussion drilling "punches" directly throughout the workpiece. Trepanning drilling involves cutting around the circumference of the hole to be generate [4-6]. In both cases the hole is obtained in few seconds (in trepanning, it was estimated about 8 minutes for a single component system, 424 holes).

In last years, there was growing interest in the use of lasers for micro cutting and micro drilling operation. Laser drilling holes in aero-engine components must comply with strict quality standard that determine them suitable for in service use. Since small diameters (0.3-1.0 mm), tight tolerances, perpendicular surfaces, no burr and no recast layer are required, the trepanning remains the most suitable technique. Many authors have studied the use of flashlamp and diode pumped Nd:YAG pulsed laser sources, focussing on the geometrical and metallurgical quality of the hole. Some negative effects of the laser drilling and cutting process, including micro-cracking, spatter, dross, and taper of the drill hole were observed [7-12]. However, this kind of laser sources operated in TEM_{00} or low-order Gaussian modes. An increase of laser power normally leads to a reduction of beam quality. In comparison to that, the beam quality of a fiber laser is independent from the output power, over a wide range. This results in a better focussing and then higher cutting speeds with comparable or better kerf quality, in term of: small dimension, spatter and dross absence, recast layer and HAZ extension. Furthermore, this characteristics are enhanced by the use of high quality short and ultrashort pulsed laser [13-18]. However, when the material thickness is limited (<1 mm), the use of a high quality fibre laser, working in CW or modulated regime, could be an economical and practical solution, as demonstrated in [19-20].

Nevertheless, since trepanning laser drilling is adopted in order to have high quality hole it is necessary to know the geometrical feature of the kerf and how they depend on the process parameters. Consequently, in this experimental study, the laser micro-cutting of NIMONIC® C236 super alloy, with the application of a single-mode fiber laser, is presented. Linear cutting tests were performed on NIMONIC® C236 sheet, 0.38 mm in thickness at the maximum pulse power (100 W), varying the pulse duration, the average power (by way of the on time) the gas pressure and the cutting speed respect to the maximum cutting speed. A full factorial design was developed according to the Design of Experiments (DoE) methodology. The kerf geometry was measured by optical microscopy according to the UNI EN 12584 2001 and ISO 9013:2002 standard.

2. Equipment, material and experimental procedures

2.1. Equipment

The cutting tests were carried adopting a 100 W Fibre Laser (SPI-RedPower SP100C), working at the wavelength, $\lambda = 1090$ nm. The laser source is transferred via an optical fibre, 6 m in length, to a laser head (from HAAS LTI) mounted on a 3+1 axis CNC system. The laser source was controlled via an external laser controller (MCA LCT3001), which allows the setting of the power (from 10% to 100% maximum nominal power) and the regime: CW or modulated. In this last case it was also possible to set the pulse frequency and the pulse duration. The laser source power, the geometric patterns and the beam speed were controlled by the CNC system. Tab. 1 shows the detailed characteristics of the laser system.

Tab. 1: Laser source characteristics (SPI -RedPower SP100C).

Parameters	Value	Unit
Wavelength	1090	[nm]
Nominal power	100	[W]
Mode operation	CW or Modulated	--
Pulse frequency	1-18	[kHz]*
Pulse duration	1-0.01 ms	[ms]*
Beam diameter ($1/e^2$)	5.0 ± 0.5	[mm]
Full angle divergence	<0.4	[mrad]
Beam Quality	TEM_{00} (M^2 <1.1)	--
	BPP 0.38	[mm.mrad]
Beam expander	0.32 X	--
Focal length	50	[mm]
Beam diameter at the focal spot	$\phi \approx 48$	[μm]
Nozzle diameter	0.8	[mm]

* in pulse regime

Tab. 2: Chemical composition and properties of NIMONIC® C263.

Element	Ni	Co	Cr	Mo	Ti	C
min [%]	Bal.	19	19	5.6	1.9	0.04
max [%]		21	21	6.1	2.4	0.08
Element	**Mn**	**Al**	**Si**	**Cu**	**Fe**	**S**
min [%]	--	--	--	--	--	
max [%]	0.60	0.60	0.4	0.20	0.07	0.007
Element	**B**	**Pb**	**Ag**	**Bi**		
min [%]	--	--	--	--		
max [%]	0.005	0.0020	0.0005	0.0001		

Physical properties	Value	Units
Density	8.36	[g/cm^3]
Melting Range		
Liquidus temperature	1355	[°C]
Solidus temperature	1300	
Specific Heat	461	[J/kg,°C]
Thermal Conductivity	11.72*	[W/m°C]
Linear Thermal Expansion,	11.0	[10-6/°C]
Mechanical properties*	**Value**	**Units**
Tensile Strength	1004**	[MPa]
Yeld Strenght (at 0.2%)	585**	[MPa]
Elongation	45**	[%]
Reduction of Area	41**	[%]
Young's modulus	221**	[GPa]
Torsional modulus	86**	[GPa]

* heat treatment: 2 h/1150°C/WQ + 8 h/800°C/AC,
** at 20 °C.

2.2. Material

The investigated material was the NIMONIC® C263 (UNS N07263/W. Nr. 2.4650) in form of rolled sheets 0.38 mm in thickness. The NIMONIC® alloy 263 was developed by Rolls-Royce (1971) Ltd. to provide a sheet material which offer improved properties in terms of proof stress and creep strength. In Table 2 the chemical composition and the main properties of NIMONIC® C263 alloy are reported.

2.3. Experimental procedures

The experimental campaign is articulated in two steps. First, in order to found the maximum cutting speed, defined as the speed after which it is not possible to cut the metal sheet, cutting pre-tests were performed at a fixed pressure value of 8 bar, changing the average power, the pulse duration and the cutting speed.

Then, in order to verify the quality of the cut and to assess the influence of the process parameters on kerf geometry, a second series of tests, with linear cuts 40mm long, was developed. For this test, a systematic approach based on a full factorial design 2^4 was adopted according to the Design of Experiments (DoE) methodology.

The adopted control factors were the following: pulse duration *d* (A), critical cutting speed percentage *Ccs* (B), gas pressure *P* (C) and average power *Pa* (D). The critical cutting speed percentage *Ccs* is the percentage of the cutting speed at a fixed average power.

The control factors were selected accordingly to the above mentioned considerations. In particular the duration and the average power (by way of the pulse frequency) were chosen in order to take into account the possible influence of the pulse-off cooling and on time effects. While, it was chose to use the *Ccs* instead the cutting speed in order to have comparable levels for the adopted different average power. Table 3 summarizes the levels of control factors and their settings. Moreover in such a table, the absolute values of the cutting speed together to the cutting speed percentage *Ccs*, was reported. Four replications for each treatment (i.e. process condition) were performed, resulting in a total of 64 experimental runs. The replications of each treatment were performed to provide more consistent response repeatability. To reduce the disturbance of any unconsidered noise factor, the order of trials was randomized both in the treatments and in their replications.

After the tests, the samples were cut by diamond saw, impregnated and polished using abrasive paper of grit size up to P2500 (Standard ISO 6344). Then, kerf geometry was measured by optical microscopy, in terms of following response variables: upper kerf width (Uk), down kerf width (Dk), tolerance (U) and taper angle (Ta).

All response variables were measured according to the UNI EN 12584 2001 and ISO 9013:2002 standard. Fig. 1 shows a sketch of the kerf section and how Uk, Dk, and U were measured.

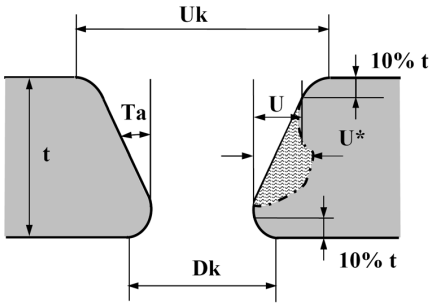

Fig. 1: Kerf geometry according to UNI EN 12584 2001 and ISO 9013:2002: upper kerf (Uk); down kerf (Dk), tolerance (U) and taper angle (Ta).

Tab. 3: Control factors and their settings.

Control factor	Label	Low (−)	High (+)	Unit
Pulse duration, *d*	A	0.05	0.4	[ms]
Critical cutting speed, *Ccs*	B	60	80	[%]
		631*	841*	[mm/min]
		1773**	2364**	
Gas pressure, *P*	C	8	12	[bar]
Average power, *Pa*	D	40	80	[W]

*Absolute values at 40W.
**Absolute values at 80W.

3. Experimental results and discussion

3.1. Maximum cutting speed

In Fig. 2 the maximum cutting speed as a function of the average power is reported at different pulse duration. So it is possible to say that in the adopted range of variable the maximum cutting speed only depends on the average power. So it was decided to perform the cutting test adopting the 80% and 60% of the maximum cutting speed for the two different average power levels.

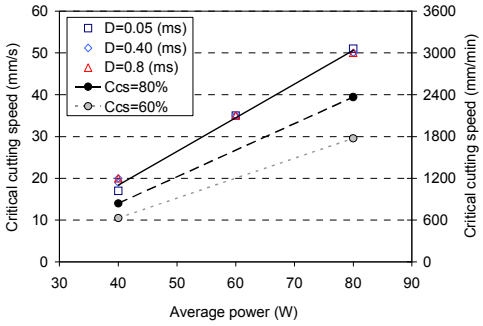

Fig. 2: Critical cutting speed as a function of average power for different duration. The circular points represent the adopted cutting speed.

3.2. Statistical analysis of results

The ANalysis Of VAriance (ANOVA) was applied in order to test the statistical significance of the main effects and the two-factor interactions for upper kerf width (Uk), down kerf width (Dk), tolerance (U) and the taper angle (Ta). The analysis was carried out at a 95 % confidence level ($\alpha = 0.05$). ANOVA assumes that the observations are normally and independently distributed with the same variance for each treatment or factor level. Before the analysis, these assumptions have been successfully checked via analysis of residuals, in agreement with what reported in [21]. However, these results were not reported here for sake of briefness. The ANOVA results are summarized in Tab. 4 in terms of *p*-values for the different response variables. On the basis of assumptions made, a control factor, or a combination of control factors, is statistically significant if the *p*-value is less than 0.05. From the table, the kerfs (both upper and down) are affected by the pressure (C), the average power (D) and by the interactions AB; the tolerance is affected by the pressure (C), and the interaction AB; while the taper angle by the duration (A) and the average power (D).

The main effect of a factor is defined as the change in response produced by a change in the level of the factor. When the difference in response between the levels of one factor is not the same at all levels of the other factors, there is an interaction between the factors. In Fig.s 3-4, the main effect and the interaction plots of all response variables taken into account are reported.

3.3. Technological interpretation

Regarding upper and down kerf width, Fig. 3a and Fig. 3b show their main effects, respectively. The significant effects are highlighted by red lines. For both of these response variables the width increases when the pressure increases and decreases when the average power increases. The function of assistant gas is to blow the molten material away from the cutting area. Obviously the greater the pressure, the more effective is the gas action. This phenomena justifies the increase of the kerf widths increasing the pressure.

Tab. 4: Result of ANOVA, *p*-value. In the table the *p*-value of the significant control factors are highlighted by bolt and underlined text.

Source	Label	Uk [µm]	Dk [µm]	U [µm]	Ta [°Deg]
d [ms]	A	0.135	0.105	0.377	**0.000**
Ccs [%]	B	0.107	0.109	0.061	0.825
P [bar]	C	**0.013**	**0.050**	**0.026**	0.599
Pa [W]	D	**0.000**	**0.022**	0.332	**0.012**
*d*Ccs*	AB	**0.016**	**0.020**	**0.039**	0.326
*d*P*	AC	0.870	0.351	0.093	0.259
*d*Pa*	AD	0.376	0.461	0.171	0.206
*Ccs*P*	BC	0.424	0.244	0.760	0.562
*Ccs*Pa*	BD	0.763	0.666	0.392	0.759
*P*Pa*	CD	0.724	0.759	0.873	0.689

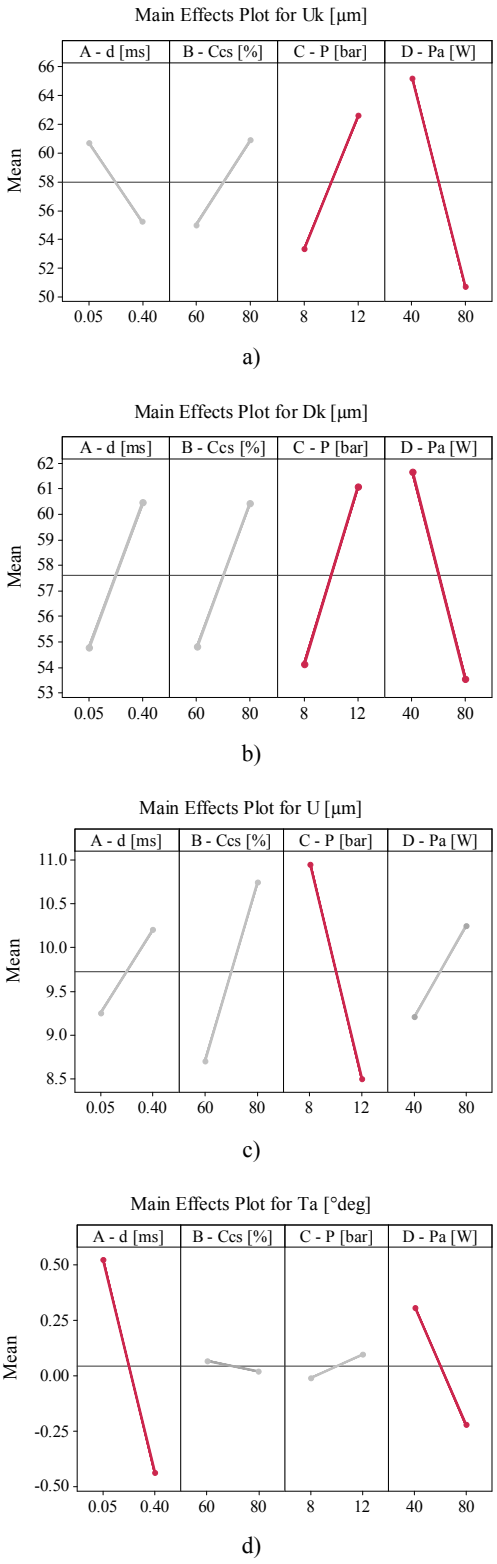

Fig. 3: Main effects plots for a) upper kerf; b) down kerf; c) tolerance; d) taper angle.

The effect of the power is not unexpected taking into account the ratio between the power and cutting speed (i.e. the energy released for unit length). Indeed, under the adopted conditions, when the laser works with the power set at the highest level (i.e. 80W) this ratio is always less than at low value (i.e. 40W), as shown in Fig. 5. Then, the decrease of the kerf widths is due to the energy released decrease.

Fig. 3c shows the main effect of tolerance (U) where tolerance decreases when pressure increases. It happens because the gas is more effective in molten material removal increasing the pressure. Consequently, a smoother surface is obtained inside the kerf. Note that U is due to typical hourglass shape of the kerf section and particularly to the down kerf enlargement as shown in Fig. 6.

Fig. 3d shows the main effects plot for taper angle (Ta). Ta decreases when pulse duration increases. It happens because, although the duration is not significant for kerf widths, Uk and Dk show an opposite behaviour at the pulse duration level change (the first decreases when the second increases). Consequently, the taper angle, that is function of difference between Uk and Dk values, is more sensitive to the duration than Uk and Dk. The effect of the power is similar. The change of the Ta is due to the difference in change of Uk and Dk. In other words: Uk changes more than Dk at the *Pa* change.

The interaction plots between *d*-*Ccs,* for Uk and Dk show anti-synergic interactions, as reported in the Fig.s 4a-4b. At the low level of duration (i.e. 0.05 ms) an increase of the *Ccs* produces a decrease of both Uk and Dk. The opposite occurs when *d* is set at the high level (i.e. 0.4 ms). This result is unexpected, since an increase of the cutting speed produces a decrease of the energy released for unit length, so a decrease in the kerf widths is expected. However, this is due to the particular regime of the adopted laser (modulated).

Due to the low peak power (i.e. 100W) and consequently low irradiance, the cutting process does not involve in cutting by vaporisation. As results, the molten removal is just due to gas action rather than the recoil pressure.

It is possible to suppose that, for long duration (i.e. 0.4 ms) and low cutting speed, the molten material tends to increase. However, the gas action is not enough to eject the molten material so it tends to settle and to solidify at the kerf input and output, producing a Uk and Dk decrease, as shown in Fig. 6.

The above mentioned behaviours explain also the interaction between duration and critical cutting speed for U, Fig. 4c. At the low level of duration (i.e. 0.05 ms), the decrease of the *Ccs* permits an enlargement of the kerf, included the middle section, and then a U reduction. At the high level of duration (i.e. 0.4 ms) this phenomena is counteracted by the solidification of the molten material that stagnates in the central section.

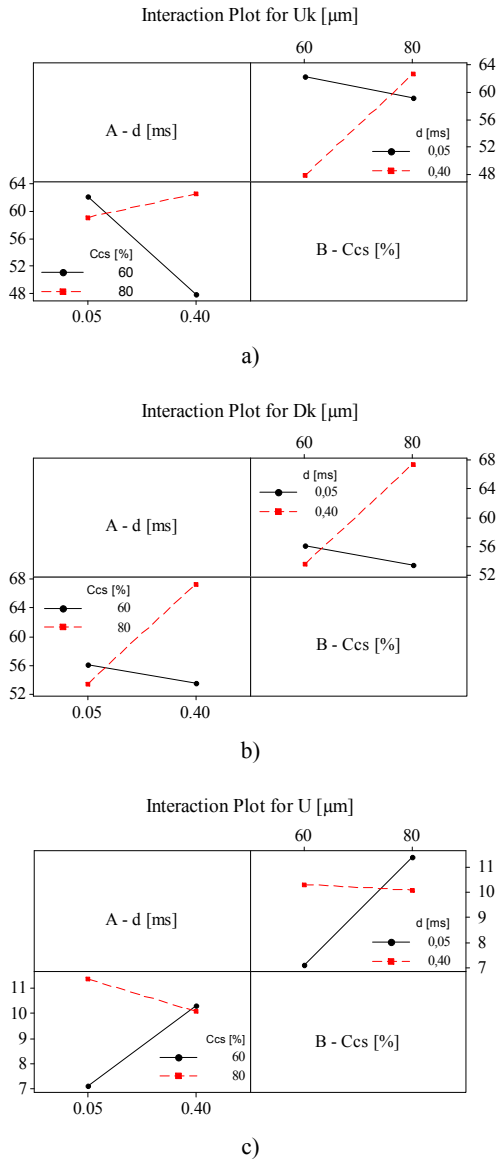

Fig. 4: Interaction plots for a) upper kerf; b) down kerf; c) tolerance.

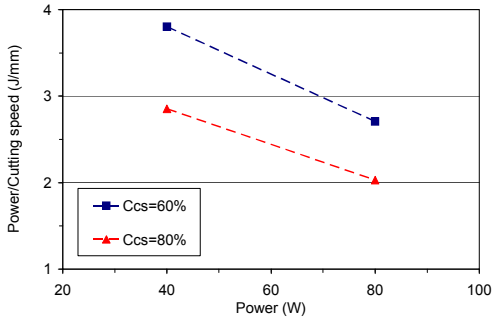

Fig. 5: Power/cutting speed ratio as a function of power and *Ccs* levels.

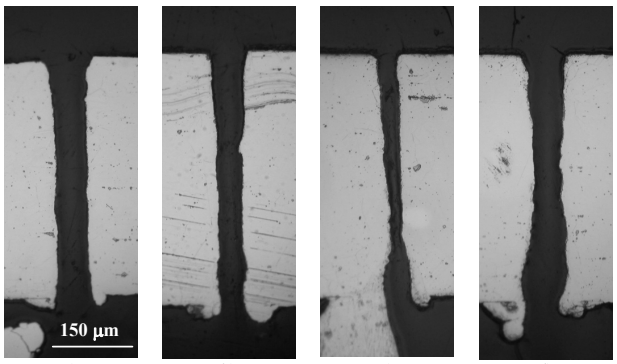

Fig. 6: Images of the kerf section obtained at *Pa*=40W. *P*=12 bar and: a) *d*=0.05 ms. *Ccs*=60%; b) *d*=0.05 ms. *Ccs*=80%; c) *d*= 0.40 ms. *Ccs*=60%; d) *d*=0.40 ms. *Ccs*=80%.

Conclusions

In this work, laser cutting of NIMONIC® C263 sheet was performed adopting a high quality beam and modulated fibre laser, in order to study the process parameters effect on kerf geometry. On the basis of the experimental campaign carried out and of the results above discussed the following conclusions can be drawn:

- the maximum cutting speed is linearly depending on the average power;
- the kerfs widths are affected by both the gas pressure and the average power. However the ratio between the power and the effective cutting speed seems to be more appropriate parameters to describe the kerf widths behaviours;
- the tolerance U is affected by the pressure while the taper angle by the duration and the average power;
- for long duration (i.e. 0.4 ms) and low critical speed percentage (*Ccs*) the gas action is not enough to expel the molten material. This tends to settle and to solidify at the kerf input and output producing a Uk and Dk decrease.

It is important to underline that the kerf widths, the tolerance and the taper angle are compatible to the requirements for the diffusion cooling system placed inside the turbine blade.

Acknowledgements

The present work was supported by the "*Ministero dello Sviluppo Economico*" of Italy as part of the PON-FIT research program. Grant No. B01/0707/01-03/X17 which is gratefully acknowledged as well as by the project *INnovazione tecnologica nei SIStemi di Trasporto* (INSIST) within the Industrial Technology Network. Theme Transportation - Aeronautics - Space as foreseen by the POR Campania FSE 2007/2013 Axis IV and V.

The authors are also grateful to *GE AVIO* for providing the material adopted in the experimentation.

References

[1] Laraia M, Manna M, Cinque G, Di Martino P. A combustor liner cooling system design methodology based on a fluid/structure approach. Applied Thermal Engineering 2013; 60: 105-121.
[2] Cerri G, Giovannelli A, Battisti L, Fedrizzi R. Advances in effusive cooling techniques of gas turbines. Appl. Therm. Eng.. 2007; 27: 692-698.
[3] Han JC, Dutta S, Ekkad SV, Gas Turbine Heat Transfer and Cooling Technology. Taylor & Francis. New York; 2000.
[4] Dhar S, Saini N, Purohit R. A review on laser drilling and its Techniques. International Conference on Advances in Mechanical Engineering AME 2006. 1-3 December 2006. Fatehgarh Sahib. Punjab. India.
[5] Ashkenasia D, Kaszemeikata T, Muellera N, Dietricha R. Eichlera HJ, Illinga G. Laser Trepanning for Industrial Applications. Physics Procedia. 2011; 12: 323-331.
[6] Jacobs P. Aerospace applications of precision trepanning. 27th International Congress on Applications of Lasers and Electro-Optics ICALEO 2008. Emecula. CA; USA; 20-23 October 2008. 2008; 168-174.
[7] Thawari G, Sarin Sundar JK, Sundararajan G, Joshi SV. Influence of process parameters during pulsed Nd:YAG laser cutting. of nickel-base superalloys. J. of Materials Processing Technology 2005; 170: 229-239.
[8] Dubey AK, Yadava V. Multi-objective optimization of Nd:YAG laser cutting of nickel-based superalloy sheet using orthogonal array with principal component analysis. Optics and Lasers in Engineering 2008; 46: 124-132.
[9] Rao R, Yadava V. Multi-objective optimization of Nd:YAG laser cutting of thin superalloy sheet using grey relational analysis with entropy measurement. Optics and Lasers in Engineering. 2009; 41: 922-930.
[10] Sibalija TV, Petronic SZ, Majstorovic VD, Prokic-Cvetkovic R, Milosavljevic A. Multi-response design of Nd:YAG laser drilling of Ni-based superalloy sheets using Taguchi's quality loss function. multivariate statistical methods and artificial intelligence. International Journal of Advanced Manufacturing Technology. 2011; 54/5-8: 537-552.
[11] Petronić S, Kovačević G, Milosavljević A, Milosavljević A, Sedmak A. Microstructural changes of Nimonic-263 superalloy caused by laser beam action. Physica Scripta. 2012; T149. Article number 014080.
[12] Morace RE, Leone C, De Iorio I. Cutting of thin metal sheets using Nd:YAG lasers with different pulse duration. Proceedings of SPIE. 2005; 6157: art. no.61570Q.
[13] Cheng-Shun Chen, Sheng-Yao Lin1, Nai-Kuan Chou, Yih-Sharng Chen, Sheau-Fan Ma1. Optimization of Laser Processing in the Fabrication of Stents. Materials Transactions. 2012; 53/11: 2023-2027.
[14] Dausinger F. Precise drilling with short pulsed lasers. Proceedings of SPIE. 2000; 3888: 180-187.
[15] Arnaboldi S, Bassani P, Biffi CA, Carnevale M, Lecis N, Lo Conte A, Previtali B, Tuissi A. Microcutting of niticu alloy with pulsed fiber laser. Biennial Conference on Engineering Systems Design and Analysis. ASME-ESDA 2010. 12-14 July 2010. Instanbul Turkey. 1: 593-602.
[16] Biffi CA, Previtali B. Spatter reduction in nanosecond fibre laser drilling using an innovative nozze. Int J. Advanced Manufacturing Technology. 2013; 66: 1231-1245.
[17] Kling R, Dijoux M, Romoli L, Tantussi F, Sanabria J, Mottay E. Metal micro drilling combining high power femtosecond laser and trepanning head. Proceedings of SPIE. 2013; 8608: Article number 86080F.
[18] Romoli L, Rashed CAA, Fiaschi M. Experimental characterization of the inner surface in micro-drilling of spray holes: A comparison between ultrashort pulsed laser and EDM. Optics and Laser Technology. 2014; 56: 35-42.
[19] Baumeister M, Dickmann K, Hoult T. Fiber laser micro-cutting of stainless steel sheets. Applied Physics A: Materials Science and Processing. 2006; 85/2: 121-124.
[20] Astarita A, Genna S, Leone C, Memola Capece Minutolo F, Paradiso V, Squillace A. Ti-6Al-4V Cutting by 100W fibre laser in both CW and modulated regime. Key Engineering Materials. 2013; V. 554-557: 1835-1844.
[21] Montgomery DC., Design and Analysis of Experiments. New York. Wiley. 2008.